

Two-state theory of single-molecule stretching experimentsFabio Manca,¹ Stefano Giordano,^{2,3,*} Pier Luca Palla,^{2,4} Fabrizio Cleri,^{2,4} and Luciano Colombo¹¹*Department of Physics, University of Cagliari, 09042 Monserrato, Italy*²*Institute of Electronics, Microelectronics and Nanotechnology (UMR CNRS 8520), 59652 Villeneuve d'Ascq, France*³*International Associated Laboratory LEMAC/LICS, ECLille, 59652 Villeneuve d'Ascq, France*⁴*University of Lille I, 59652 Villeneuve d'Ascq, France*

(Received 7 May 2012; revised manuscript received 9 November 2012; published 8 March 2013)

We present a statistical mechanics analysis of the finite-size elasticity of model polymers, consisting of domains that can exhibit transitions between more than one stable state at large applied force. The constant-force (Gibbs) and constant-displacement (Helmholtz) formulations of single-molecule stretching experiments are shown to converge in the thermodynamic limit. Monte Carlo simulations of continuous three-dimensional polymers of variable length are carried out, based on this formulation. We demonstrate that the experimental force-extension curves for short and long polymers are described by a unique universal model, despite the differences in chemistry and rate-dependence of transition forces.

DOI: [10.1103/PhysRevE.87.032705](https://doi.org/10.1103/PhysRevE.87.032705)

PACS number(s): 87.15.A–, 83.10.Gr, 87.15.La

I. INTRODUCTION

Dynamic force spectroscopy by means of the atomic-force microscope (AFM), laser- or magnetic-tweezers apparatus, or the biomembrane force probe allows the direct probing of the elasticity of individual molecules, and as such has rapidly become a mainstay of biophysical research [1–4]. These mechanical devices are quite different from one another, one prominent difference being their equivalent stiffness, in the range of $10^{-4} - 1$ pN/nm for tweezers, versus $10 - 10^2$ pN/nm for the AFM [4]. The typical experiment is a mechanically induced unfolding of a biological polymer made of N domains, e.g., a polysaccharide such as dextran [5], a protein such as titin [6], a DNA or RNA strand [7], and so on. As a function of increasing force levels, different mechanical response regimes are observed, beginning with the entropic unfolding of the polymer chain, now well understood in terms of simple worm-like chain (WLC) or freely jointed chain (FJC) models [8]; to the linear-elastic extension of the straightened chain; to the so-called *overstretching*, typically interpreted as a conformational transformation of the domain geometry; up to the eventual fracturing of the polymer.

Several theoretical models have been introduced to shed light on the force-induced transformations, notably in DNA. For example, a macroscopic thermodynamics analysis led to a *melting* interpretation of the overstretching transition [9], with *double-strained* DNA (dsDNA) separating into noninteracting *single-strained* DNA (ssDNA) strands. This model was subsequently extended in order to consider different conditions of temperature, pH, and ionic strength [10]. However, a more recent thermodynamics analysis [11] compared DNA melting with the conformational transformation from dsDNA to a supposed *stretched*-DNA, or S-DNA form, and found the latter to be in much better agreement with available experimental data. However, recent experimental results show that when the content of Adenine-Thymine (AT) pairs is high, a force-induced denaturation (melting) is observed; by contrast, sequences with a prevalence of Guanine-Cytosine

(GC) pairs are found to undergo an overstretch transition into a distinct base-paired form [12]. Comparisons of experimental results with *ad-hoc* models have been also drawn for analyzing structural transitions of simultaneously twisted and stretched DNA molecules [13]. Some other general properties of bistable systems have been studied through the Fermi-Pasta-Ulam chain model [14,15], by a two-state FJC polymer [16,17], and by the so-called discrete persistent chain that borrows features from both the FJC and the WLC chain models [18]. Also, atomic-scale computer simulations based on molecular dynamics have been used to analyze physicochemical details of different polymers and biomolecules: as an example concerning the DNA mechanics, it has been shown that the double helix can be extended to twice its normal length before its base pairs break [19]. Moreover, the force needed to completely separate the two strands has been numerically determined [20], and some noncanonical forms generated by DNA stretching and compression have been predicted [21].

In spite of the richness of experimental results and the large number of models devoted to explain specific situations, a universal theoretical approach able to describe the different observed responses is not yet available. Typically, the experimental results can be subdivided in two separated classes showing cooperative and noncooperative mechanically induced unfolding. Any of the above-discussed polymer models is able to explain only one of these two observed responses. We are, therefore, interested in developing a unifying model capturing at the same time the main features of both behaviors.

In this context, we provide a robust microscopic statistical mechanics foundation to the interpretation of the overstretching regime (or conformational transitions regime), which we describe in terms of the internal dynamics of a chain of two-state systems undergoing a conformational transformation, as described by the double-well potential in Fig. 1. For the sake of argument we call “folded” and “unfolded” the two conformations; however, the transformation occurs, more generally, between two principal local minima of the domain free-energy hypersurface (e.g., for DNA it could as well represent the melting transition [22]). Then, we first develop a theoretical model describing experiments at constant applied force (a realization of Gibbs ensemble statistics) and we show

*stefano.giordano@iemn.univ-lille1.fr

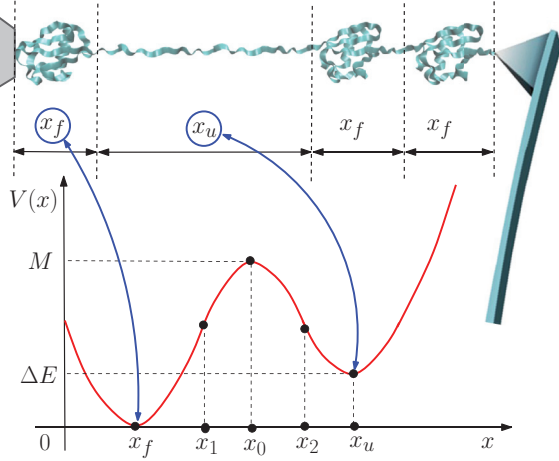


FIG. 1. (Color online) Potential energy function with an energy barrier. Folded and unfolded configurations of the domains are schematically represented.

that the conformational change must occur simultaneously for all the domains at a given threshold force.

On the other hand, experiments performed at constant displacement are a realization of the Helmholtz ensemble of statistical mechanics. In our previous work [23], we showed that the outcome of the two types of experiment converge in the thermodynamic limit of infinite chain length, $N \rightarrow \infty$. Moreover, the equivalence of the different statistical ensembles in the thermodynamic limit (for Gaussian polymers and chains of rigid rods) is largely discussed in Ref. [24]. On the contrary, if the thermodynamic limit is not reached, it has been shown that different boundary conditions (Helmholtz and Gibbs ensembles) imposed for stretching the polymer lead to different force-extension curves [23–27]. In practice, real experiments always fall in between these two ideal extremes. Therefore, here we focus on the intermediate cases described by finite values of the k_c/k ratio, k and k_c being the equivalent spring constant (i.e., stiffness) of the domain and of the pulling device, respectively. We demonstrate by means of Monte Carlo simulations that the typical “sawtooth” pattern [6], observed for the unfolding of large protein domains (such as the Ig units in titin), and the “plateau” or kink [5,7], observed in the overstretching of DNA and polysaccharides (e.g., dextran), have a common origin in the size-dependence of the polymer response to the external force, the plateau shape being attained in the limit of large N . On the same grounds, at a fixed number N of domains, the transition from the “plateau” (cooperative) to the “sawtooth” (noncooperative) response is recovered for increasing values of k_c/k . Notably, such a behavior of the force-extension curves is universal with respect to the specification of any additional parameters, such as chemical, structural, or mechanical constants of the domains.

II. THEORETICAL MODEL AND CALCULATIONS

We work out a simple model containing the minimal ingredients fully describing the overall complex behavior of a polymer chain. It consists of an N -domain, nonbranched chain clamped at one end, able to describe conformational transitions across an energy barrier. The internal state of

each domain is described by a potential energy $V(x)$, which exhibits two minima corresponding to the lengths $x = x_f$ (folded conformation) and $x = x_u$ (unfolded conformation), connected via an energy barrier M at $x = x_0$ (see Fig. 1). The energy is written as a C^2 piecewise function, constructed by imposing continuity and differentiability at the joining points x_1 and x_2 :

$$V(x) = \begin{cases} \frac{1}{2}k(x - x_f)^2 & 0 < x < x_1 \\ -\frac{1}{2}k(x - x_0)^2 + M & x_1 < x < x_2 \\ \frac{1}{2}k(x - x_u)^2 + \Delta E & x > x_2. \end{cases} \quad (1)$$

For chosen values of the lengths x_f and x_u , the domain spring constant k , and the energy difference ΔE between the two conformations, the other parameters are simply given by: $\delta = x_u - x_f$, $x_0 = (x_u + x_f)/2 + 2\Delta E/(k\delta)$, $M = (k/4)[\delta/2 + 2\Delta E/(k\delta)]^2$, $x_1 = x_f + \delta/4 + \Delta E/(k\delta)$, and $x_2 = x_u - \delta/4 + \Delta E/(k\delta)$. Therefore, this model properly gives a barrier with $x_f < x_0 < x_u$ only for $|\Delta E| \leq k\delta^2/4$. The model is based on the equilibrium statistical mechanics and, therefore, it should be applied to the case of very slow stretching cycles or for all transitions occurring much faster than the characteristic velocity of the experiment.

A. The Gibbs ensemble: Cooperative response

Upon application of a constant force f to the end of the polymer identified by the position vector $\vec{r}_N = (x_N, y_N, z_N)$ (the other end being fixed in the origin), the statistics of the fluctuating chain is a realization of the Gibbs ensemble [23]. The partition function in thermodynamic equilibrium is given by $Z_f(f, T) = \int_{\Gamma_N} e^{-\tilde{h}/k_B T} dq^N dp^N$, with $\Gamma_N = R^{6N}$. The augmented Hamiltonian \tilde{h} includes the classical kinetic energy of the domains with mass m , their total potential energy, and a term, $-fz_N$, describing the applied force along the z axis [23]. In the framework of the present minimal model, the partition function can be explicitly calculated as

$$Z_f(f, T) = \left(\frac{2\pi m}{\beta}\right)^{3N/2} \left(\frac{2\pi}{\beta f}\right)^N [\Pi(\beta k, \beta f, x_f, 0, x_1) + e^{-\beta M} \Pi(-\beta k, \beta f, x_0, x_1, x_2) + e^{-\beta \Delta E} \Pi(\beta k, \beta f, x_u, x_2, +\infty)]^N, \quad (2)$$

with $\beta = (k_B T)^{-1}$ and

$$\Pi(\alpha, \gamma, x_0, a, b) = 2 \int_a^b x e^{-\frac{\alpha}{2}(x-x_0)^2} \sinh(\gamma x) dx. \quad (3)$$

The function Π can be written as

$$\Pi(\alpha, \gamma, x_0, a, b) = I(\alpha, \gamma, x_0, a, b) - I(\alpha, -\gamma, x_0, a, b), \quad (4)$$

where the integral I can be calculated in closed form

$$I(\alpha, \gamma, x_0, a, b) = \int_a^b x e^{-\alpha(x-x_0)^2} e^{\gamma x} dx = e^{\gamma x_0} e^{\frac{\gamma^2}{4\alpha}} \left\{ \frac{1}{2\alpha} (e^{-A^2} - e^{-B^2}) + \sqrt{\frac{\pi}{\alpha}} \frac{\gamma + 2\alpha x_0}{4\alpha} [\text{Erf}(B) - \text{Erf}(A)] \right\}, \quad (5)$$

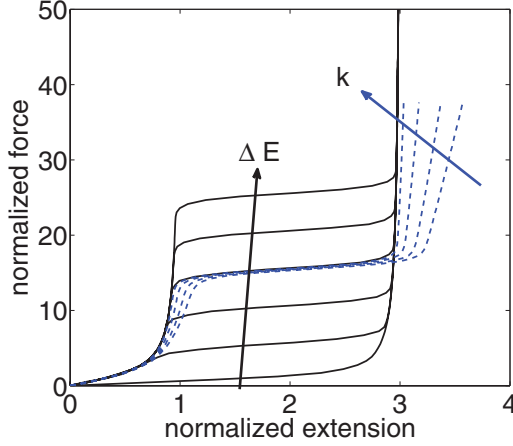


FIG. 2. (Color online) Force-extension curves for the Gibbs ensemble: normalized force f/f_β vs. normalized extension $r/(Nx_f)$. The black solid lines correspond to different values of the energy $\Delta E = 0, 10, 20, 30, 40, 50 k_B T$ (increasing values from the bottom up) for a fixed spring constant $k = 2000 k_B T/(\text{nm})^2$. The blue dashed lines correspond to different values of the spring constant $k = 10, 15, 30, 100 k_B T/(\text{nm})^2$ (increasing values from the right to the left) for a fixed value of the energy barrier $\Delta E = 30 k_B T$.

with

$$\mathcal{A} = \sqrt{\alpha} \left(a - x_0 - \frac{\gamma}{2\alpha} \right), \quad \mathcal{B} = \sqrt{\alpha} \left(b - x_0 - \frac{\gamma}{2\alpha} \right). \quad (6)$$

The extension r at a given force is obtained from the partition function as $r = k_B T (\partial \log Z_f / \partial f)$. Since the extension is linearly dependent on N , the data for chains of different lengths can be scaled to a single curve upon dividing by N .

Figure 2 shows the results of the normalized force-extension curves, f/f_β (where $f_\beta^{-1} = \beta x_f$), in terms of $r/(Nx_f)$ for different values of the energy barrier $\Delta E = 0, 10, 20, 30, 40, 50 k_B T$ (black solid lines) at a fixed value of $k = 2000 k_B T/(\text{nm})^2$, and for different values of the spring constant k (blue dashed lines) at a fixed value of $\Delta E = 30 k_B T$. As an example, we also adopted $x_u = 3x_f$ or, equivalently, $\delta = 2x_f$. Both sets of curves display a force plateau at $f \simeq \Delta E/\delta$, for any $\Delta E > 0$, with a normalized width equal to δ . In our model, the plateau indicates a transition in the polymer conformation, meaning that for $f < \Delta E/\delta$ each domain is found in the folded conformation at $x = x_f$, while for $f > \Delta E/\delta$ domains are in the unfolded conformation at $x = x_u$; i.e., the ensemble of domains respond *cooperatively* to the external force. Notably, the value of the plateau force inducing the conformational transition does not depend on the spring constant, k , nor on the temperature. Such a result is readily interpreted in the framework of the Bell expression [28], as the threshold value of force necessary to make the unfolding rate equal to the (reverse) folding one, i.e., lowering the difference ΔE to zero.

As an example of application, in the case of dsDNA, which displays a plateau at $f = 65 \text{ pN}$ with a $\delta \approx 2.4 \text{ \AA}$, our criterion gives an energy estimate $\Delta E = 3.8 k_B T$. Here, the value of f is the observed transition force and the parameter δ represents the measured length rise per base pair in the transition from dsDNA to its stretched version (experimentally estimated [7,22] to be a factor of ~ 1.7 larger than the normal value of 3.4 \AA [29,30]). It turns out that the above theoretical

$\Delta E = 3.8 k_B T$ fits quite well with the available experimental data [22,31]. On the other hand, the difference of extension between dsDNA and ssDNA is characterized by a smaller factor of ~ 1.5 [7] and the energetic difference ΔE is about $2.5 k_B T$ (per base pair) [32,33]. Since $2.5 k_B T < 3.8 k_B T$ the process should be interpreted as a melting transition (at lower energy and therefore preferred). As a matter of fact, there is a wide debate on the interpretation of the dsDNA transition by means of a melting process or through the emerging of a stretched (S-DNA) structure; the problem is still awaiting conclusive experimental evidences. In our context we have simply used the experimental data $(f, \Delta E, \delta)$ of the transition, which are valid independently of the real nature of the process. To further show the complexity of this problem, we also note that it has been recently approached by analyzing the behavior of DNA sequences with controlled base content [12]. It has been proved that when the AT content is around 70% the application of a force of about 62 pN generates a denaturation (melting) with an extension factor of ~ 1.7 . Conversely, sequences with GC content of 60%, under the same force, show a reversible transition into a new stable structure extent by a factor ~ 1.5 [12]. Unfortunately, no energetic data are available to make a comparison with our theory.

A similar plateau was observed for other long chain polymers, such as dextran with $N = 275$, $x_f = 0.5 \text{ nm}$, $x_u = 0.56 \text{ nm}$, $\Delta E = 13.2 k_B T$ [5], for which the simple criterion $f \approx \Delta E/\delta$ gives plateau forces in the range of $\approx 900 \text{ pN}$, as indeed observed [34].

From the theoretical point of view, another description of the cooperative response can be found in Refs. [16–18]. Nevertheless, our formulation is appropriate to obtain the force-extension curves also under Helmholtz conditions, as described below.

B. The Helmholtz ensemble: Noncooperative response

While Gibbs ensemble statistics are sampled with a constant applied force, a dual situation can be realized by imposing the extension, i.e., by controlling the polymer end-to-end distance. The statistics of the fluctuating polymer in this latter scheme is a realization of the Helmholtz ensemble. As shown in Ref. [23], the corresponding partition function Z_r cannot be written in closed form and, as opposed to the Gibbs case, the corresponding extension r is nonlinearly dependent on N . However, we showed that the partition functions in the two ensembles are formally related via a Laplace transform, and we demonstrated [23] that they lead to a common force-extension curve in the thermodynamic limit.

It should be noted that any AFM or tweezers experiment falls in an intermediate regime between the two ideal extremes, of purely constant force or constant extension, since either constraint on the terminal domain of the chain is mediated by a mechanical device (such as the AFM cantilever, or the laser-bound microsphere, plus a molecular spacer providing adhesion). The device is characterized by its own effective elastic constant k_c , which is coupled in series to the chain of domain springs k . In the limit of a soft device, $k_c/k \rightarrow 0$, the statistics of the coupled system reduces to the Gibbs ensemble for the isolated molecule fluctuating under a constant force. On the other hand, for a very stiff device, $k_c/k \rightarrow \infty$, one

recovers the Helmholtz ensemble for the isolated molecule held at a fixed extension by the fluctuating force [35].

To describe such a situation, we adopt a Monte Carlo (MC) numerical approach, simulating the stretching of the chain produced by a device with a proper adjustable elastic stiffness. Compared to previous MC simulations of the polymer stretching [36–39], we adopted a scheme ensuring a very efficient exploration of the bimodal configuration space [40,41]. While in the Metropolis method one usually adopts a single step size for each MC move [23], in the present simulations we added a second step size, equal to $\delta = x_f - x_u$ [40]. The first step size is used for most moves, while the second one is sampled for a small fraction of the moves, ensuring the overcoming of the barrier at any temperature, while still preserving the detailed balance [41].

In Fig. 3, top panel, we report the results of the MC simulations at $T = 293$ K, for decreasing values of the k_c/k ratio, from 0.05, that is well within the Helmholtz statistics regime, down to 1×10^{-4} , i.e., approaching Gibbs ensemble statistics. The remaining parameters are set to $N = 4$, $\Delta E = 30 k_B T$, $x_f = 2.5$ nm, $x_u = 3x_f$, and $k = 100 k_B T/\text{nm}^2$,

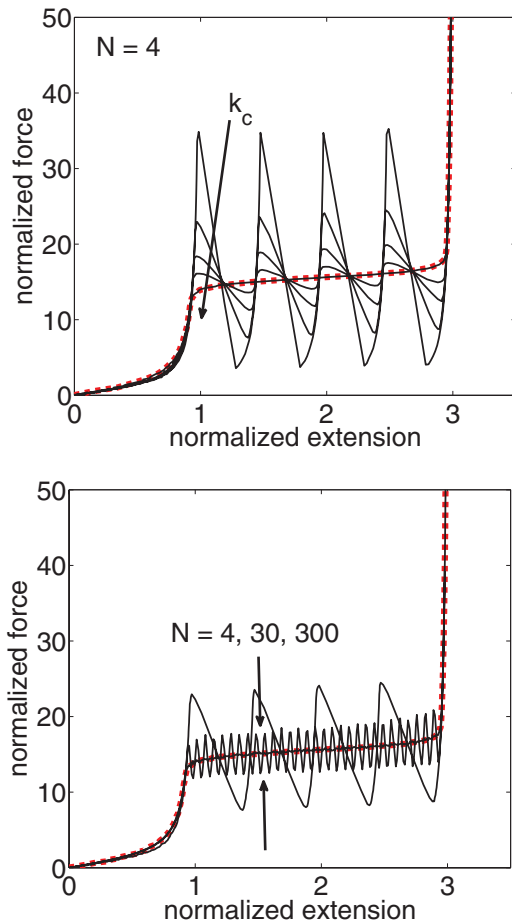


FIG. 3. (Color online) Monte Carlo force-extension curves at $T = 293$ K, for: (top panel) different decreasing values of the device spring constant $k_c = 5, 2, 1, 0.5, 0.01 k_B T/(\text{nm})^2$ (from the top down) and $N = 4$; (lower panel) increasing number of domains $N = 4, 30, 300$ with $k_c = 2 k_B T/(\text{nm})^2$ (bottom panel). The red dashed line corresponds to the Gibbs ensemble. The remaining parameters are $\Delta E = 30 k_B T$, $x_f = 2.5$ nm, $x_u = 3x_f$, and $k = 100 k_B T/(\text{nm})^2$.

which can be considered representative of a medium-sized, multidomain chain protein. At large values of k_c/k , the domains exhibit a sequence of *independent* conformational transitions to the unfolded configuration, generating a series of N peaks (sawtooth pattern), which closely resemble the experimental results obtained for short chains (e.g., a titin fragment with $N = 8$, $x_f = 4$ nm, $x_u = 32$ nm, $\Delta E = 11.1 k_B T$ [34]). For $k_c/k \rightarrow 0$, the peak-to-valley width, Δf , of the sawtooth shrinks and the curve approaches the $k_c = 0$ cooperative plateau of Gibbs statistics. In substantial agreement with this finding, pulling experiments on native titin by means of optical tweezers [42], having a very small equivalent k_c compared to the AFM one, do not reveal the sawtooth pattern, but rather a smooth, monotonic branch reminiscent of the horizontal plateau.

On the other hand, a similar asymptotic trend is observed (Fig. 3, bottom panel) when the chain length, i.e., the number of domains, is increased, at a fixed value of k_c/k . As N increases, the width Δf is decreased until, at a large enough N , the force-extension curves approach again the plateau curve of the Gibbs ensemble. It is worth noting that a similar trend was observed in experiments performed on native titin, comprising several hundreds of Ig domains, for which the width Δf was of the order of 80 pN [6], compared to the much shorter 8-monomer titin, for which $\Delta f > 200$ pN. The experiments performed on dextran, a long polysaccharide with $N = 275$ [5,34], whose response to the applied force shows a plateau closer to the typical DNA-like behavior, can also be rationalized on this basis. In summary, we proved that the macroscopically different behavior of small- N polymers (such as titin) versus long polymers (such as dextran, DNA), as well as experiments done on a same polymer but with devices having widely different stiffness, can be interpreted with the very same unifying model, interpolating between the two extremes of pure Gibbs or Helmholtz statistics.

A similar dependence of the results on the type of loading devices has been found in recent literature for a one-dimensional chain of bistable elements [14,15]: the authors prove that the system “snaps” for a soft device, while it “pops” for a hard device. Our results extend these previous ones by considering thermal fluctuations in the whole three-dimensional space.

As observed by several authors, each branch of the sawtooth pattern can be nicely fitted by a sequence of FJC, or WLC curves (see Fig. 4, left panel, dashed lines) with a proper value of the persistence length, up to the unfolding of each domain (see, e.g., titin [6], spectrin [43], fibronectin [44], synaptotagmin [45]). Beyond this point, the force relaxes to a smaller value, until the next curve is met and the force can start rising again upon increasing displacement. By considering Fig. 4 (left panel), we determine the position r_n of the peaks as follows: in correspondence of the n th peak, we have $n - 1$ domains in the unfolded configuration (extension x_u) and $N - n + 1$ domains in the folded configuration (extension x_f). Therefore,

$$\frac{r_n}{Nx_f} = 1 + \frac{(n-1)(x_u - x_f)}{Nx_f}, \quad (7)$$

for $n = 1, \dots, N$ ($n = N + 1$ corresponding to the final asymptote). We also note that the increasing parts of the

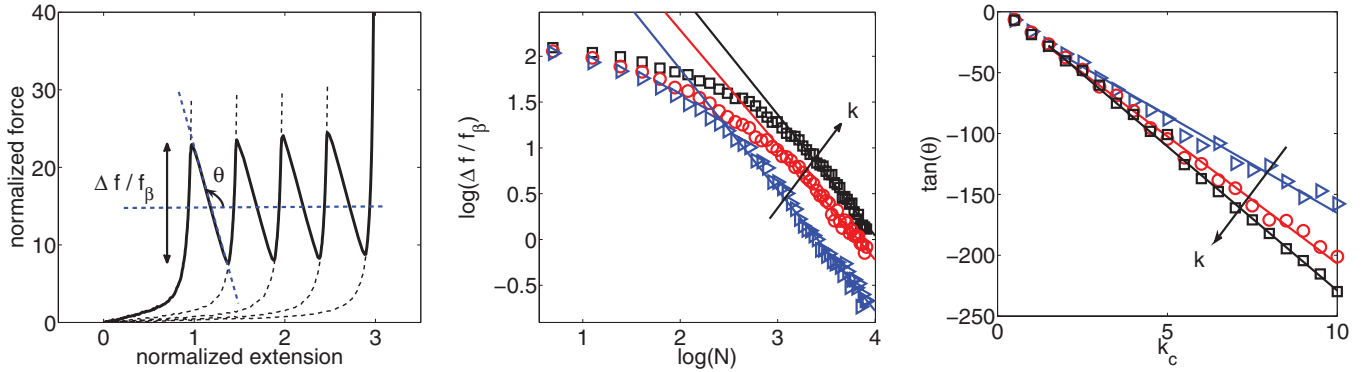


FIG. 4. (Color online) Left panel: definition of Δf and θ for a typical force-extension curve with $N = 4$. Dashed lines for the growing branches fitted to FJC with increasing contour length. Central panel: plot of $\log(\Delta f/f_\beta)$ vs. $\log(N)$ for $k_c = 1 k_B T / (\text{nm})^2$ and $k/k_c = 20, 30, 100$ (blue, red and black lines, respectively; we used natural logarithms). Right panel: plot of $\tan(\theta)$ vs. k_c for $N = 4$ and the same k values. Remaining parameters: $\Delta E = 30 k_B T$, $x_f = 2.5 \text{ nm}$, $x_u = 3x_f$ and $T = 293 \text{ K}$.

force-extension curve (dashed lines in Fig. 4, left panel) can be represented by polymers with N domains described by simple harmonic potentials $V(x) = (1/2)k(x - r_n/N)^2$.

Since the physical origin of the growing branch of the curves is well understood on the basis of FJC or WLC models, we analyzed the decreasing branch, as identified by the common width Δf and angle θ in Fig. 4 (left panel), which were extracted from our MC simulations as a function of N and k_c/k .

By looking at Fig. 4 (center), the peak-to-valley width shows a power-law decrease with the chain length, $\Delta f \sim N^{-\alpha}$, the exponent $\alpha = 1.3$ being remarkably independent on the k_c/k ratio. This finding indicates that attainment of the thermodynamic limit is mainly dictated by the thermal force scale, f_β , and to a much lesser extent by other structural and chemical details of the polymer. It is worth noting that the value of the exponent is in agreement with previous results on monostable FJC and WLC models with extensible bonds [23].

The last plot on the right of Fig. 4 reports the behavior of $\tan(\theta)$ as a function of the device stiffness, k_c . The observed linear dependence is another remarkable result, completely describing the transition between the two extremes (Gibbs and Helmholtz ensembles), while taking into account all the intermediate cases. For $k_c/k \rightarrow \infty$, we have $\tan(\theta) \rightarrow -\infty$ or, equivalently, $\theta \rightarrow \pi/2$. In other words, the decreasing

branches of the force-extension curve must be exactly vertical in the case of the Helmholtz ensemble. Notably, both the values of Δf and θ are fully prescribed; i.e., the entire shape of the force-extension curve is uniquely defined, once the free parameters of the model are specified.

III. CONCLUSIONS

In conclusion, we described the statistical mechanics of chain polymers composed by domains with two stable states, subject to a pulling force by a molecular-scale mechanical device. We showed that for short chain length, or large stiffness of the device, the domain response is uncorrelated and originates the typical sawtooth force-extension curve observed in many experiments. On the other hand, upon increasing chain length, or vanishing device stiffness, the response is cooperative and results in the plateau-like curve, also observed in other experiments. Despite the simplicity of the model, such a framework provides a unified picture for such apparently contrasting experimental situations.

ACKNOWLEDGMENTS

F.M. acknowledges the University of Cagliari for the extended visiting grant and the IEMN UMR CNRS 8520, University of Lille I, for the kind hospitality.

- [1] F. Ritort, *J. Phys.: Condens. Matter* **18**, R531 (2006).
- [2] F. Cleri, *Sci. Model. Simul.* **15**, 369 (2008).
- [3] K. R. Chaurasiya, T. Paramanathan, M. J. McCauley, and M. C. Williams, *Phys. Life Rev.* **7**, 299 (2010).
- [4] K. C. Neuman and A. Nagy, *Nature Meth.* **5**, 491 (2008).
- [5] M. Rief, F. Oesterhelt, B. Heymann, and H. E. Gaub, *Science* **275**, 28 (1997).
- [6] M. Rief, M. Gautel, F. Oesterhelt, J. M. Fernandez, and H. E. Gaub, *Science* **276**, 1109 (1997).
- [7] S. M. Smith, Y. Cui, and C. Bustamante, *Science* **271**, 795 (1996).
- [8] J. F. Marko and E. D. Siggia, *Macromolecules* **28**, 8759 (1995).
- [9] I. Rouzina and V. A. Bloomfield, *Biophys. J.* **80**, 882 (2001).
- [10] I. Rouzina and V. A. Bloomfield, *Biophys. J.* **80**, 894 (2001).
- [11] S. Cocco, J. Yan, J.-F. Léger, D. Chatenay, and J. F. Marko, *Phys. Rev. E* **70**, 011910 (2004).
- [12] N. Bosaeus, A. H. El-Sagheer, T. Brown, S. B. Smith, B. Akerman, C. Bustamante, and B. Nordén, *Proc. Natl. Acad. Sci. USA* **109**, 15179 (2012).
- [13] J. F. Léger, G. Romano, A. Sarkar, J. Robert, L. Bourdieu, D. Chatenay, and J. F. Marko, *Phys. Rev. Lett.* **83**, 1066 (1999).
- [14] G. Puglisi and L. Truskinovsky, *J. Mech. Phys. Sol.* **48**, 1 (2000).

- [15] Y. R. Efendiev and L. Truskinovsky, *Continuum Mech. Thermodyn.* **22**, 679 (2010).
- [16] H. J. Kreuzer and M. Grunze, *Europhys. Lett.* **55**, 640 (2001).
- [17] F. Hanke and H. J. Kreuzer, *Eur. Phys. J. E* **22**, 163 (2007).
- [18] C. Storm and P. C. Nelson, *Phys. Rev. E* **67**, 051906 (2003).
- [19] A. Lebrun and R. Lavery, *Nucleic Acid Res.* **24**, 2260 (1996).
- [20] M. W. Konrad and J. T. Bolonick, *J. Am. Chem. Soc.* **118**, 10989 (1996).
- [21] K. M. Kosikov, A. A. Gorin, V. B. Zhurkin, and W. K. Olson, *J. Mol. Biol.* **289**, 1301 (1999).
- [22] P. Cluzel, A. Lebrun, C. Heller, R. Lavery, J.-L. Viovy, D. Chatenay, and F. Caron, *Science* **271**, 792 (1996).
- [23] F. Manca, S. Giordano, P. L. Palla, R. Zucca, F. Cleri, and L. Colombo, *J. Chem. Phys.* **136**, 154906 (2012).
- [24] R. G. Winkler, *Soft Matter* **6**, 6183 (2010).
- [25] J. H. Weiner and M. R. Pear, *Macromolecules* **10**, 317 (1977).
- [26] D. Keller, D. Swigon, and C. Bustamante, *Biophys. J.* **84**, 733 (2003).
- [27] S. Sinha and J. Samuel, *Phys. Rev. E* **71**, 021104 (2005).
- [28] G. I. Bell, *Science* **200**, 618 (1978).
- [29] C. R. Calladine, H. R. Drew, B. F. Luisi, and A. A. Travers, *Understanding DNA: The Molecule and How It Works* (Elsevier Academic Press, Amsterdam, 2004).
- [30] W. Saenger, *Principles of Nucleic Acid Structure* (Springer-Verlag, New York, 1984).
- [31] A. Ahsan, J. Rudnick, and R. Bruinsma, *Biophys. J.* **74**, 132 (1998).
- [32] J. J. SantaLucia, *Proc. Natl. Acad. Sci. USA* **95**, 1460 (1998).
- [33] J. J. SantaLucia and D. Hicks, *Annu. Rev. Biophys. Biomol. Struct.* **33**, 415 (2004).
- [34] M. Rief, J. M. Fernandez, and H. E. Gaub, *Phys. Rev. Lett.* **81**, 4764 (1998).
- [35] H. J. Kreuzer and S. H. Payne, *Phys. Rev. E* **63**, 021906 (2001).
- [36] W. T. King, M. Su, and G. Yang, *Int. J. Biol. Macromol.* **46**, 159 (2010).
- [37] A. R. Singh, D. Giri, and S. Kumar, *J. Stat. Mech.* (2011) P05019.
- [38] F. Manca, S. Giordano, P. L. Palla, F. Cleri, and L. Colombo, *J. Phys.: Conf. Ser.* **383**, 012016 (2012).
- [39] F. Manca, S. Giordano, P. L. Palla, F. Cleri, and L. Colombo, *J. Chem. Phys.* **137**, 244907 (2012).
- [40] R. Q. Topper *et al.*, *Rev. Comp. Chem.* **19**, 1 (2003).
- [41] D. D. Frantz, D. L. Freeman, and J. D. Doll, *J. Chem. Phys.* **93**, 2769 (1990).
- [42] M. S. Kellermayer, S. B. Smith, H. L. Granzier, and C. Bustamante, *Science* **276**, 1112 (1997).
- [43] M. Rief, J. Pascual, M. Saraste, and H. E. Gaub, *J. Mol. Biol.* **286**, 553 (1999).
- [44] A. F. Oberhauser, C. Badilla-Fernandez, M. Carrion-Vazquez, and J. M. Fernandez, *J. Mol. Biol.* **319**, 433 (2002).
- [45] M. Carrion-Vazquez, A. F. Oberhauser, T. E. Fisher, P. E. Marszalek, H. Li, and J. M. Fernandez, *Prog. Biophys. Mol. Biol.* **74**, 63 (2000).